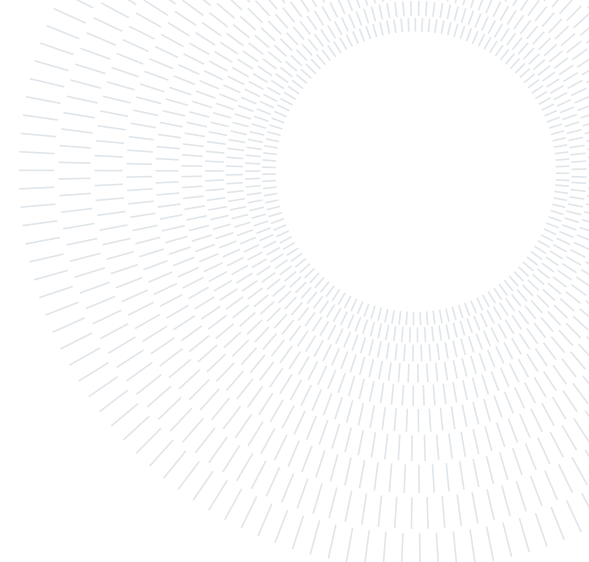




**POLITECNICO**  
**MILANO 1863**

**SCUOLA DI INGEGNERIA INDUSTRIALE  
E DELL'INFORMAZIONE**



EXECUTIVE SUMMARY OF THE THESIS

## Design of a lattice-based cooling jacket for electric in-wheel motors manufactured by Laser Powder Bed Fusion

LAUREA MAGISTRALE IN MECHANICAL ENGINEERING - INGEGNERIA MECCANICA

**Author:** LORENZO SERVENTI

**Advisor:** PROF. STEFANO FOLETTI

**Co-advisor:** PROF. ALI GÖKHAN DEMIR

**Academic year:** 2021-2022

---

### 1. Introduction

The Dynamis PRC team is the racing car division of the Politecnico of Milano. The team competes in a car design competition called Formula SAE, alongside with universities from all over the world. In 2019 – 2020 season, Dynamis team developed its first electric vehicle. The new designed car adopts four different electric in-wheel motors placed outside the car body, directly connected to the wheel hubs. Due to space limitations and challenging thermal management, motor cooling is crucial to maintain high motor efficiency. The cooling system component in charge to keep the motor in optimal working conditions is an external cooling jacket placed around each motor. This project tries to further develop the design of this specific component starting from Dynamis design.

The most common cooling jackets consist of an external cylindrical metal single shell placed around the electric motor[1]. A gap is left between the motor surface and the component shell, allowing a coolant fluid to flow directly in contact with the hot motor surface to subtract its generated thermal power. According to the internal geometry design, the fluid flow is forced to follow a specific path in this gap.

The best compromise between heat dissipation capabilities and flow pressure drop is given by an helical fluid flow path extending along the component axial direction. The helical pattern of the water flow is guaranteed by internally manufactured thin walls that develop helically on the inside part of the cooling jacket. The heated fluid is then sent and cooled in a liquid – air radiator and to a pump to repeat the cycle. Leakages are prevented by properly designed gaskets. This component can also reject thermal power to the surrounding environment due to the interaction with ambient air stream, relieving workload from the whole cooling system. A proper external fin arrangement can be designed to improve this additional thermal exchange. Figure 1 shows the component mounted on the electric motor, with Dynamis external rectangular fin system. Due to geometry complexity of the component, it has been decided to take advantage of the intrinsic versatility of Laser Powder Bed Fusion (LPBF) manufacturing technique. In LPBF, a high power laser selectively melts small metal particles into a final 3-dimensional shape. LPBF recreates a part layer by layer along a growth direction. Aluminium powder is used due to its good heat conduction capabil-

ities and mechanical properties.

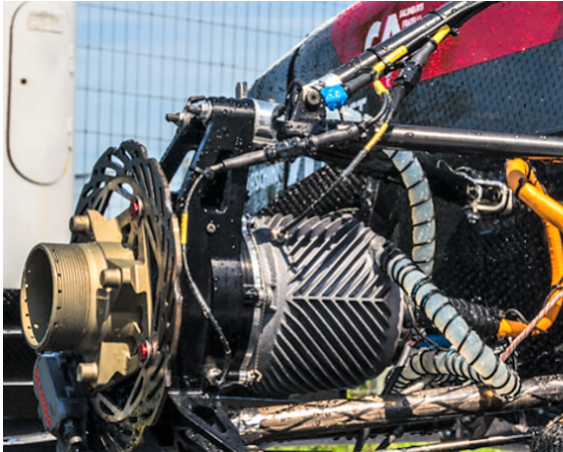


Figure 1: Dynamis cooling jacket for season 2019 - 2020 mounted on front left motor.

## 2. State of the Art

Performances of a cooling jacket, and in general of heat exchangers, are mainly summarised by its pressure loss and by the heat transfer capability [2]. Pressure loss can be qualitatively seen as the resistance that the fluid encounters while flowing through the jacket. The more the fluid is obstructed or is subjected to quick changes in direction, the higher the pressure losses. This would lead to higher pumping power demand, reducing the electric power that the battery can be delivered to the motors. On the other hand, fluid turbulence and induced mixing are beneficial for heat transfer. An efficient design must consider both these performance indicators and balance their effects. Literature studies have been carried out to understand the influence of turbulence promoters and lattice structures as a mean to increase thermo-hydraulic performances of the cooling jackets.

### 2.1. Strut-based lattice structures in heat transfer applications

Strut-based lattice structures are "topologically ordered, three-dimensional open-celled structures composed of one or more repeating unit cells. These cells are defined by the dimensions and connectivity of their constituent strut elements, which are connected at specific nodes." [3]. These structures attractiveness comes from their lightness and high surface area, while keeping an overall simple design. Particular interest is reserved to the tetrahedral unit cell due

to the extensive experimental and numerical research of its application as a mean to enhance heat transfer performance [4]. The tetrahedral unit cell is constituted by three struts forming a pyramid with equilateral triangular base.

The most relevant conclusions from heat transfer point of view on the interaction of a fluid flow with an heated lattice structure are that flow mixing and turbulence increase the convective heat transfer. Vortexes formation around heated struts disturbs the flow boundary layer and enhances heat transfer performance. Moreover, the extension of total heat transfer surface due to heat conduction through the lattice further increases convection to the fluid flow.

However, the pressure drop increases with higher flow blockage and generated vorticity. The optimal solution compromises between these two aspects. These conclusions are not only valid for tetrahedral cell and lattice structures, but also for other heat transfer enhancing techniques such as spherical dimples in the flow channel [5]. Having in mind the possible advantages of additional features, they can be applied to the cooling jacket both in the internal water channel and on the external side to replace existing fins to enhance component performances.

## 3. Design of the cooling jacket

The design phase can be divided into two distinguished areas: the internal channel and the external fins. The final solution is considered to be the combination of the best performing internal and external configurations.

### 3.1. Internal geometry

As discussed in Chapter 2, the cooling jacket will adopt the single shell configuration with circumferential water flow around the motor. The height of the internally manufactured thin walls that guide the water flow determines the water channel height, which is the distance between the component single shell and motor surface. Due to limited computational power availability and complexity of studied solutions, the helical channel that envelops the electric motor has been divided into curved sectors that have been studied separately. Hence, to simplify modelling procedure and analysis, the different internal channel configurations are compared using only the first sector encountered by the incoming cold

water. A single sector is then considered to be representative of the whole internal channel, allowing to directly compare various solutions in an easier way. Another assumption made is that curved sectors can be converted to planar sectors having the same dimensions, assuming that performances will only slightly change. The modelling procedure would be highly simplified, still allowing direct comparison between different internal geometries. This assumption was proved numerically, performances for the same geometry differ within 5%.

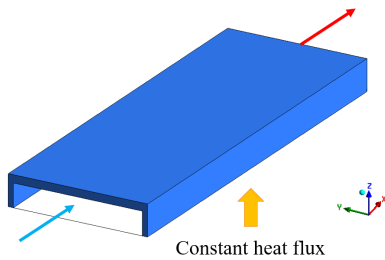


Figure 2: Model of the empty channel with 4.5 mm of water.

Figure 2 shows the model of a 75 mm long 25 mm wide planar sector. The blue part represents the solid domain, with a portion of the single shell and the two lateral internal flow guiding walls. The transparent domain is the fluid, with inlet and outlet walls. Heat is introduced by setting a constant heat flux boundary condition on the water surface directly in contact with the motor. Having analysed only a sector instead of the whole water channel, the following statements are considered to choose the best performing solution:

- The total pressure loss of the whole cooling jacket is obtained by applying the linearity assumption as the sum of the consecutive pressure drops of all the sectors in which the jacket is divided. All the sectors of the same cooling jacket have the same geometry and inlet velocity boundary condition, so the pressure drop is assumed to be the same for all of them. From this point of view, the best channel design is the one with less pressure drop.
- From heat transfer point of view, the convective heat transfer coefficient of the first sector encountered by incoming water is used to select the best configuration. It is defined as:

$$h = \frac{\dot{q}}{T_{surface} - T_{ref}} \quad (1)$$

It depends on the heat flux  $\dot{q}$  provided from the motor to the water and on the temperature difference between unperturbed fluid flow  $T_{ref}$  and the interface temperature  $T_{surface}$ . The best channel design is the one with highest  $h$ , hence lowest  $T_{surface}$ .

The investigated geometries have been:

- Empty channel with 2, 3, 4.5, 6 mm water thickness
- Spherical dimples in 3, 4.5, 6 mm water thickness
- 3 mm high tetrahedral cells in 4.5, 6 mm water thickness, shown in Figure 3
- 2 mm high tetrahedral cells in 3 mm water thickness, with 0.4 and 0.6 mm strut diameters

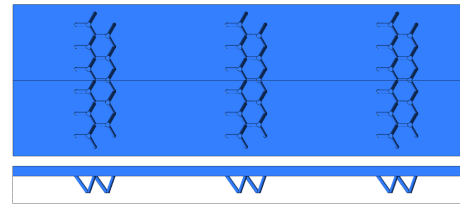


Figure 3: Model of 4.5 mm water channel with 3 mm high tetrahedral cells.

### 3.1.1 Results and conclusions

As a starting point, the empty channel is studied by varying channel thickness. Keeping fixed the water flow rate at 5 l/min and channel width, water velocity decreases as channel height increases. A slower flow in a thicker channel is better from pressure drop point of view, but the thermal transfer effectiveness is lower and motor temperature is therefore higher. On the other hand, a fast flow in a narrow channel produces high pressure drop but thermal performances improve. A trade-off velocity is required to balance these two opposing objectives.

The main idea now is to embed with dimples and cells in the channel to promote fluid mixing and turbulence. The thermal boundary layer that naturally forms on motor surface should be disturbed and convection from solid hot surface to fluid should increase. Most significant results are shown in Figure 4. The graph shows  $\Delta P$  and  $h$  for each geometry. The best performing solution is closer to bottom-right spot in the graph.

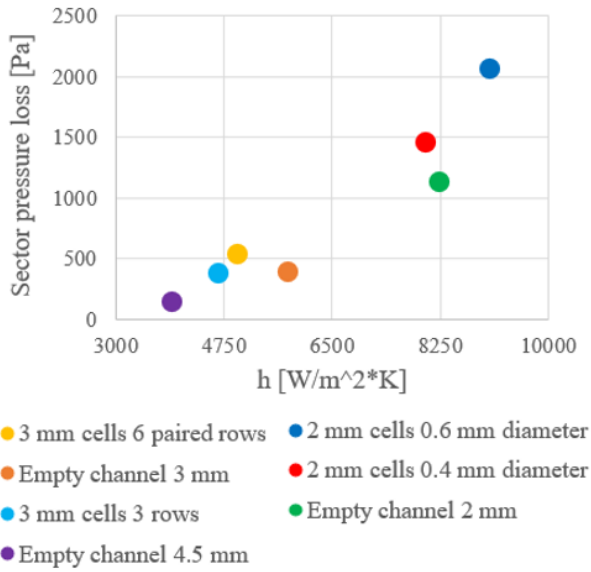


Figure 4: Internal geometries comparison.

Spherical dimples give minor improvement on heat transfer capabilities and slightly increase sector pressure loss. For fixed dimple dimension, their effect decreases at increasing channel thickness. They are not the best solution for this application and are not reported in Figure 4. Both 2 and 3 mm high tetrahedral cells highly alter performances of the empty channel thickness with same height. Their flow mixing effect is much higher compared to dimples. Convection is enhanced at the cost of higher flow blockage. The most promising solutions were the 2 mm high empty channel and the 3 mm high empty channel with 2 mm high cells with 0.4 mm strut diameter. The final choice was on the 2 mm thick empty channel since it showed slightly better performances and an easier manufacturing.

### 3.2. External geometry

The second design objective is to develop an effective external fin arrangement to have a beneficial heat rejection from the cooling jacket to the ambient air. Starting from Dynamis solid fins solution shown in Figure 1, the idea is to apply lattice structure on the outside of the cooling jacket. Taking advantage of lattice structure cells porosity and an additional wing, the air flow through cells could be conveyed to the rear part of the jacket. In this way, rear fins contribution to heat transfer would be more effective. Modelling the complete external geometry of the cooling jacket was possible only for the most simple geometries, those involving no fins and

10 mm high tetrahedral unit cells. For the other more complex lattices, a smaller planar sector was modelled to allow a lattice comparison. The tested solutions are:

- Complete jacket with no fins.
- Complete jacket with 10 mm high tetrahedral unit cells and wing.
- Axial jacket sector with tetrahedral and Octet unit cells and wing.
- Planar sectors with Tetrahedral, Octet and two variants of diamond cells.

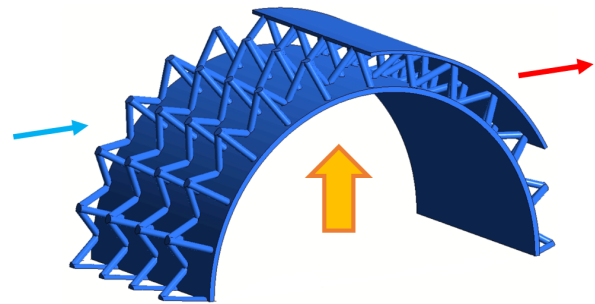


Figure 5: Tetrahedral cells fins with wing.

Figure 5 shows the complete model with tetrahedral unit cells. The model exploits both axial and radial symmetries. Air flows around the component and interacts with cells. Heat is provided from the inner surface of the component, directly from the internally flowing heated water. A constant temperature boundary condition is set on the solid - liquid interface. Different simulations have been run to understand thermal performances at varying velocities. Figure 6 shows the side view of planar sectors, modelled due to excessive geometric complexity of full model with lattice structure. They give a comparison of all the lattices. In order:

- 10 mm high tetrahedral unit cells with 2 mm strut diameter, relative density 5.4%.
- Octet unit cells, 5 mm edge, 0.6 mm strut diameter, relative density 7.3%.
- Diamond unit cells, 2 cells in sector height, 1 mm strut diameter, relative density 7.3%. It is referred as "Diamond 5 mm".
- Diamond unit cells, 1 cell in sector height, 1.35 mm strut diameter, relative density 7.3%. It is referred as "Diamond 10 mm".

The substantial difference with the complete jacket model is that in these planar sectors air is constrained and forced to go through the cells, independently from the flow blockage given by the geometry.

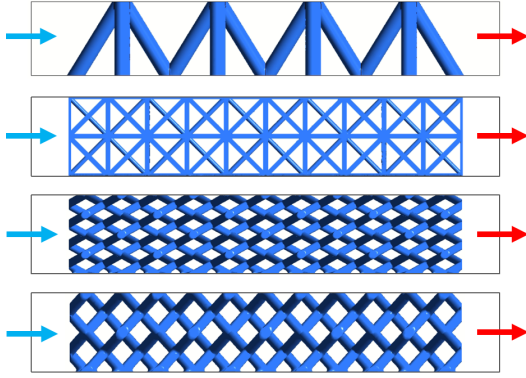


Figure 6: Planar domains.

The complete jacket model is more loyal to reality since air is free to divert when it encounters high blockage cells. Only a portion of the main stream would in fact enter the lattice structure. Geometries that are difficult to penetrate such as the Octet cell would experience a lower internal air flow, thus lower interaction and convection, compared to the planar sector models. For every planar model, the heat is introduced by imposing a constant temperature boundary condition on the planar bottom surface. The comparison of different solutions is made in terms of:

- Convective heat transfer coefficient from the heated solid to the air flow, defined as in equation (1). Now the variables are both the heat flux  $\dot{q}$  through the solid - air interface and the average interface temperature  $T_{surface}$ . Their values depends on the effects combinations of conduction and convection. The convective heat transfer coefficient comparison tells which solution, for the same interface area, is the best one in promoting heat convection from solid to ambient air. It can be seen as an effectiveness coefficient for external fin geometry.
- Total thermal power rejected to environment. This absolute value for comparison of the different solutions is calculated as:

$$Q = \dot{q}A_{interface} \quad (2)$$

where  $\dot{q}$  is the heat flux through the solid - air interface and  $A_{interface}$  is the solid - air interface area extension.

- Additional mass of external fins compared to the smooth solution with no fins. The objective is to find a geometry that provides good thermal management with additional mass as low as possible.

- For the planar sectors, the pressure loss is important to understand the flow blockage given by the geometry. The higher the blockage, the lower would be the effective air flow inside cells in the real application.

### 3.2.1 Results and conclusions

Figure 7 shows the comparison of jacket with no fins, tetrahedral cells with wing and Dynamis fins. Results of thermal power rejected have been normalized by Dynamis maximum value. Tetrahedral cells show a significant improvement compared to no fin solution. Results are comparable with Dynamis, especially at lower speed. The wing is actually able to divert the air flow through the cells to the rear part of the component. Moreover, this solution performs similarly to Dynamis solution with an overall 45.6% fins weight reduction.

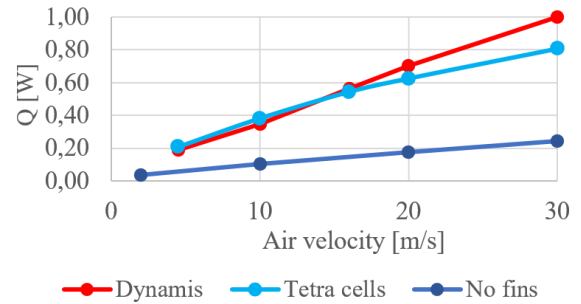


Figure 7: Comparison with Dynamis fins.

Planar sectors results are summarised in table 1.

Model	$h$ [W/m <sup>2</sup> K]	$Q$ [W]	$\Delta P$ [Pa]
Tetra cells	148,95	7,10	121,05
Octet cells	184,03	16,12	573,70
Diam. 5 mm	219,27	11,87	361,24
Diam. 10 mm	227,92	13,60	345,34

Table 1: Comparison of planar sectors.

The increase in strut diameter is positive to have a good heat conduction through the lattice to the cells top. The enhanced conduction determines an higher interface surface temperature, which leads to higher surface heat flux  $\dot{q}$  from the component to the air flow. However, high diameter geometries generally have lower total heat transfer area compared to the thinner struts cells such as Octet and 5 mm diamond cells, which is detrimental for total thermal power rejected.

The convective heat transfer coefficient  $h$ , similar for both diamond geometries, is higher compared to both tetrahedral unit cells and Octet cells results. The effectiveness of diamond geometries in promoting convection seems higher than the other solutions. The total thermal power rejected to ambient is lower for the tetrahedral cells, higher for the Octet cells, similar and intermediate for the diamond geometries. The sector pressure drop is an index of the ease for the air to enter and cross the planar sectors. Results are similar for both diamond geometries, showing a clear decrease compared to the Octet cells solution. This means that for the real application the air would enter more easily and in greater quantity in a diamond lattice structure compared to Octet cells structure. Total thermal power rejection to ambient highly depends also on the amount of air that interacts with the structure. The apparent advantage on thermal power rejected by Octet cells over the diamond cells planar sectors could disappear in the real world application. The 5 mm diamond geometry has been selected to be the external fin configuration. The weight of the last three geometries increases from the tetrahedral cells solution, but their application would still make a solution 38.7% lighter than Dynamis fins.

#### 4. LPBF process

To understand and verify the processability of the externally applied 5 mm Diamond cells structure, different samples have been prepared for the LPBF process using Autodesk Netfabb.

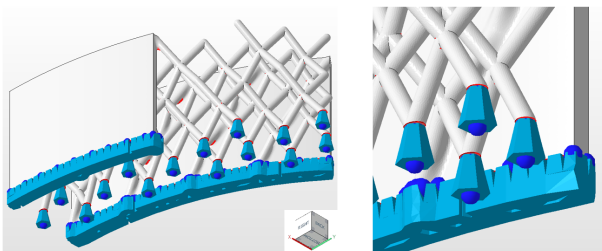


Figure 8: 5 mm diamond cells sample with wing.

The sample reported in Figure 8 represents a round sector spacing  $40^\circ$  of the total component circumference. It consists of 5 mm diamond cells geometry with a portion of the single shell on which they are embedded and a portion of the wing. Build direction coincides with jacket axial direction. Supports are depicted in blue.

#### 5. Conclusions

The proposed final design is given by the combination of the best performing solutions for the two design fields. For the internal part it is a 2 mm empty channel arranged in helical path around the motor. For the external part, a 10 mm thick lattice structure layer applied around the component made by 5 mm diamond cells with wings to deflect air in the rear part. Even though the direct comparison of the complete model with Dynamis fins was only possible for tetrahedral cells geometry, the 5 mm diamond cells show advantages in planar sector comparison. Further studies on the complete model with 5 mm diamond cells external geometry are required to allow direct comparison with Dynamis results. The proposed solution leads to a weight reduction of 38.7% compared to the Dynamis fins. Cell shape and dimension optimization could further improve thermal performances.

#### 6. Acknowledgements

I would like to thank Professors Foletti and Demir for the precious teachings and availability.

#### References

- [1] Peixin Liang, Feng Chai, Ke Shen, and Weiguo Liu. Water jacket and slot optimization of a water-cooling permanent magnet synchronous in-wheel motor. 57(3):2431–2439.
- [2] Inderjot Kaur and Prashant Singh. State-of-the-art in heat exchanger additive manufacturing. 178:121600.
- [3] Tobias Maconachie, Martin Leary, Bill Lozanovski, Xuezhe Zhang, Ma Qian, Omar Faruque, and Milan Brandt. SLM lattice structures: Properties, performance, applications and challenges. 183:108137.
- [4] T. Kim, H.P. Hodson, and T.J. Lu. Contribution of vortex structures and flow separation to local and overall pressure and heat transfer characteristics in an ultralightweight lattice material. 48(19):4243–4264.
- [5] P. M. Ligrani, M. M. Oliveira, and T. Blaskovich. Comparison of heat transfer augmentation techniques. 41(3):337–362.